Analysis of Open-Loop Timing Advance Errors in LEO Satellite Communications

Sunghoon Shim and Haejoon Jung

Department of Electronics and Information Convergence Engineering
Kyung Hee University
Yongin-si, 17104, South Korea
{tjdgns169, haejoonjung}@khu.ac.kr

In-Ho Lee

School of Electronic and Electrical Engineering
Hankyong National University
Anseong 17579, South Korea
ihlee@hknu.ac.kr

Abstract-In low-Earth orbit (LEO) satellite communication systems, the rapid relative movement between satellites and user equipment (UEs). While 3GPP Release 17 defines an openloop timing advance (TA) method that uses location information obtained through a Global Navigation Satellite System (GNSS) fix and ephemeris, the estimated TA may differ from the actual propagation delay because the UE continues to move even after the GNSS provides a fix. This paper analyzes timing errors in the GNSS fix-based open-loop TA method through simulations assuming various UE movement scenarios, including linear, circular, and zigzag. For linear and circular movements, it exceeds the maximum timing error tolerance time defined by 3GPP for subcarrier spacing (SCS) of 30 kHz. For zigzag movement, we observe that errors approach the maximum timing error tolerance time. Therefore, this study confirms the limitations of the open-loop method and emphasizes the need for additional correction techniques to achieve accurate synchronization.

I. INTRODUCTION

Non-terrestrial networks (NTNs) are gaining considerable attention as a key technology that can provide communication services in disaster areas, deserts, oceans, and polar regions, where building terrestrial infrastructure is difficult [1]–[7]. Low Earth orbit (LEO) satellites, which move quickly in orbit at a low altitude, are expected to play an important role in future NTN communication environments due to their ability to provide low latency and high data transmission rates [8]–[12].

Accurate time synchronization between user equipment (UE) and satellites is essential for stable connections in LEO-based satellite communication systems. In particular, for orthogonal frequency division multiplexing (OFDM)-based waveforms, if transmission and reception timings are out of sync, inter-symbol interference (ISI) may occur, which significantly degrades communication quality. To prevent this, all UEs must apply time alignment (TA) when transmitting uplink data. However, maintaining precise synchronization is challenging in LEO satellite communication environments due to the rapid changes in relative positions between satellites and terminals [13].

In 3GPP Release 17, the UE can use GNSS data to determine its position and calculate TA based on the ephemeris provided by the network [14]. However, obtaining GNSS signals to calculate position, known as a GNSS fix, is difficult to reflect in real time. Since the UE continues to move

after the fix, the TA calculated based on previous position information may differ from the actual value. For this reason, open-loop TA estimation results in cumulative errors that are subject to the terminal's speed, movement path, and GNSS fix intervals. These errors significantly affect communication quality, especially in highly mobile environments. Therefore, investigating TA errors considering the terminal's movement characteristics is essential.

For this reason, in this paper, we delve into the characteristics of time synchronization errors caused by the periodic GNSS fix-based open-loop TA method under various UE mobility scenarios in LEO satellite communication systems through simulation. The simulation results confirm that TA error accumulation varies depending on the UE's mobility patterns and suggest the need for additional correction techniques to achieve precise synchronization in the future [15].

II. SYSTEM MODEL

In this paper, we consider a LEO satellite communication system, where each UE is assumed to identify its position through GNSS fixes at regular intervals. The ephemeris is assumed to be provided by the network, by which the UE can estimate the location of the LEO satellite. Hence, based on this information, the uplink open-loop TA value can be calculated. Suppose that $t_{\rm fix}$ is the time at which the UE obtains its position information using the most recent GNSS signal. At a certain time before the next GNSS fix, denoted by $t_{\rm obs}$, where $t_{\rm obs} > t_{\rm fix}$, the satellite's position is defined as ${\bf s}(t_{\rm obs})$. The UE's actual position is denoted by ${\bf u}(t_{\rm obs})$, while the estimated position at the latest GNSS fix is indicated by ${\bf \hat{u}}(t_{\rm fix})$.

The open-loop TA is computed based on the UE's position at the GNSS fix time, using the estimated distance to the satellite as

$$\hat{d}(t_{\text{obs}}) = \|\mathbf{s}(t_{\text{obs}}) - \hat{\mathbf{u}}(t_{\text{fix}})\|. \tag{1}$$

Then, the estimated propagation delay and the open-loop TA value are calculated as

$$\hat{\tau}(t_{\text{obs}}) = \frac{\hat{d}(t_{\text{obs}})}{c},\tag{2}$$

$$\widehat{TA}(t_{\text{obs}}) = 2 \cdot \hat{\tau}(t_{\text{obs}}), \tag{3}$$

where c is the speed of light. However, since the actual UE continues to move after $t_{\rm fix}$, the actual distance and propagation delay can be expressed as

$$d(t_{\text{obs}}) = \|\mathbf{s}(t_{\text{obs}}) - \mathbf{u}(t_{\text{obs}})\|, \qquad (4)$$

$$\tau(t_{\text{obs}}) = \frac{d(t_{\text{obs}})}{c}.$$
 (5)

Thus, the actual open-loop TA value is given by

$$TA(t_{obs}) = 2 \cdot \tau(t_{obs}). \tag{6}$$

Accordingly, the TA error is defined as

$$\varepsilon(t_{\text{obs}}) = \tau(t_{\text{obs}}) - \hat{\tau}(t_{\text{obs}})$$

$$= \frac{\|\mathbf{s}(t_{\text{obs}}) - \mathbf{u}(t_{\text{obs}})\|}{c} - \frac{\|\mathbf{s}(t_{\text{obs}}) - \hat{\mathbf{u}}(t_{\text{fix}})\|}{c}.$$
(7)

This TA error, $\varepsilon(t_{\rm obs})$, varies depending on the UE's movement path and speed; thus, this paper considers various UE movement scenarios to investigate their impact. We assume that the GNSS fixes are updated at regular intervals, while satellites are assumed to move at a constant speed in circular orbits at an altitude of $600~\rm km$.

III. UE TRAJECTORIES

In this paper, we present the following three movement scenarios to analyze the error of the GNSS fix-based open-loop TA method according to various movement patterns of the UE. In all scenarios, GNSS fixes occur at five-second intervals. During these intervals, TA is calculated based on the UE's position at the last fix point.

1) **Linear Trajectory**: The UE moves in a straight line at a constant speed of 60 m/s in the *y*-axis direction, as shown in Fig. 1(a), while the *x* and *z* coordinates remain constant. The equation for the linear motion model is as follows:

$$\mathbf{u}(t) = [0, \ v_{\text{UE}} \cdot t, \ r_E],\tag{8}$$

where r_E denotes the Earth's radius, while $v_{\rm UE}$ corresponds to the UE's speed.

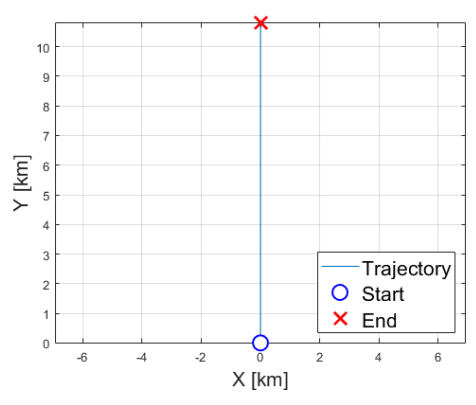
2) Circular Trajectory: The UE moves in a circular orbit with radius R at a constant speed, as shown in Fig. 1(b). Based on the total distance traveled $L = v_{\rm UE} \cdot t_{\rm total}$, the radius of the circle is set as $R = L/2\pi$. The formula for the circular motion model is as follows:

$$\mathbf{u}(t) = [R\cos(\omega t), R\sin(\omega t), r_E], \tag{9}$$

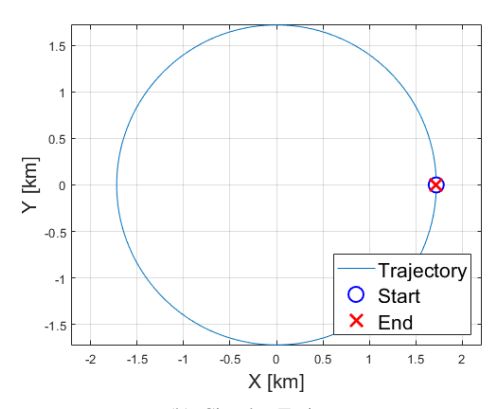
where $\omega = v_{\rm UE}/R$ is the angular speed.

3) **Zigzag Trajectory**: The UE moves diagonally along both the *x*-axis and *y*-axis as shown in Fig. 1(c), reversing the direction of movement along the *x*-axis at regular intervals to form a zigzag trajectory. The zigzag movement model is given by:

$$\mathbf{u}(t) = \left[u_x(t-1) + \alpha \cdot \frac{v_{\text{UE}}}{\sqrt{2}} \cdot t, \ u_y(t-1) + \frac{v_{\text{UE}}}{\sqrt{2}} \cdot t, \ r_E \right],$$
(10)



(a) Linear Trajectory



(b) Circular Trajectory

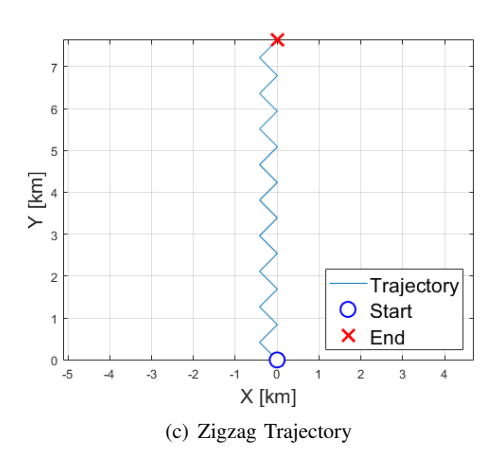


Fig. 1. UE movement trajectories

where α is a coefficient representing the x-axis direction, initially set to $\alpha=-1$, and then its sign is reversed every 10 seconds.

IV. SIMULATION RESULTS

In this simulation, we consider a LEO satellite moving along a circular orbit at an altitude of $600~\rm km$ and a UE moving at a constant speed of $60~\rm m/s$ on the ground. At the simulation start time t_0 , the satellite is positioned directly above the UE. The UE's movement trajectory consists of three scenarios: linear,

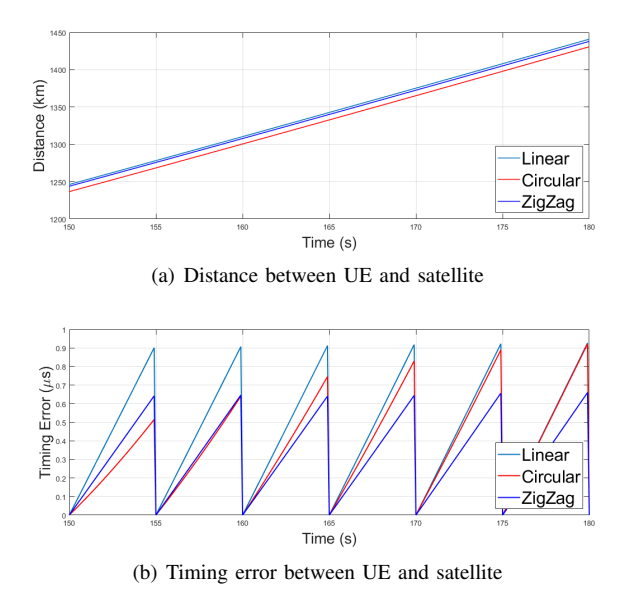


Fig. 2. Distance variation and timing error for the three UE movement scenario.

circular, and zigzag. GNSS fixes occur at five-second intervals. At each fix, the open-loop TA is estimated by calculating the round-trip propagation delay to the satellite based on the UE position at the last GNSS fix. The timing error is defined as the difference between the true value $TA(t_{\rm obs})$ and the estimated value $TA(t_{\rm obs})$.

Fig. 2(a) shows the actual distance variation between the UE and the satellite during the 150–180 second interval. While the distance generally increases due to the satellite's orbital motion, the amount of change varies depending on the UE trajectory. In the linear scenario, the UE moves in a straight line in the opposite direction of the satellite, resulting in the most rapid increase in relative distance and thus the largest timing error. The zigzag trajectory includes movement along the x-axis, reducing the effective distance change. The circular scenario exhibits varying distance change depending on the arc segment of the movement.

Fig. 2(b) illustrates the timing error over time under the open-loop TA method for the three trajectories. The error resets every 5 seconds with each GNSS fix but accumulates between the fix points. Among the three, the linear scenario resulted in the most significant error accumulation, followed by circular and zigzag in descending order.

Fig. 3 compares the root mean square error (RMSE), maximum error, and standard deviation of the timing errors across the three movement scenarios. The RMSE of the linear trajectory was the highest at approximately $0.41\mu s$, while circular and zigzag trajectories are lower at around $0.29\mu s$. In terms of the maximum error, the linear and circular scenarios yield relatively high values of approximately $0.93\mu s$ and $0.92\mu s$, respectively. Regarding standard deviation, the linear scenario shows the greatest standard deviation at $0.25\mu s$, while the zigzag scenario gives the most stable error distribution at approximately $0.17\mu s$.

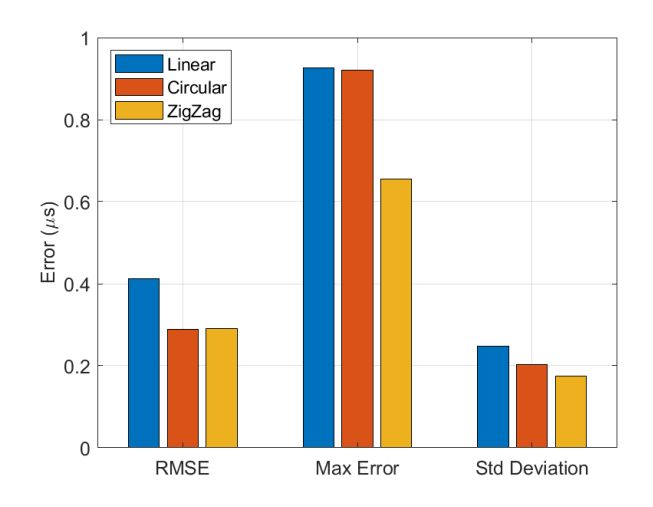


Fig. 3. Comparison of TA error metrics (RMSE, Max error, Std. deviation) across movement scenarios.

V. CONCLUSIONS AND FUTURE DIRECTIONS

In this paper, we analyzed the effect of cumulative position errors during GNSS fix intervals on open-loop-based TA calculations in various UE movement scenarios within a LEO satellite communication environment. Simulation results demonstrated that changes in the relative distance between the satellite and the UE vary depending on the UE's movement trajectory, resulting in different levels of accumulated timing error.

In particular, in the case of linear movement, the relative distance increased rapidly as the UE moved in a straight line in the opposite direction of the satellite's movement, resulting in the largest timing error. In the case of zigzag movement, which included an x-axis component, the relative distance change was smaller than in the linear case. For the circular trajectory, the relative distance varied depending on the section of the arc path. Numerically, the maximum errors for the linear and circular trajectories were approximately $0.93\mu s$ and $0.92\mu s$, respectively. These values are close to the maximum allowable timing error of $0.94\mu s$ defined by 3GPP for the SCS 15kHz standard, and exceed the $0.72\mu s$ limit set for the SCS 30kHz configuration. These results indicate that accurate synchronization cannot be guaranteed under certain conditions when relying solely on the open-loop TA approach.

Therefore, this study confirms the necessity of a TA correction that accounts for the GNSS fix interval and the UE's movement pattern. It also suggests that a robust synchronization framework should incorporate auxiliary mechanisms, such as the closed-loop correction method [16] and estimation techniques based on the extended Kalman filter (EKF), as in [17] and [18].

ACKNOWLEDGEMENT

This work was supported by the MSIT, Korea, in part under the National Research Foundation of Korea grant (RS-2023-00303757 and RS-2022-NR069055), in part under the ITRC support programs (IITP-2025-RS-2021-II212046), and in part under the Convergence security core talent training business support program (IITP-2023-RS-2023-00266615) supervised by the IITP.

REFERENCES

- "Cooperative transmission of UAV swarm using orthogonal time-frequency space modulation," *ICT Express*, vol. 10, no. 6, pp. 1240–1246, 2024.
- [2] B. You, I.-H. Lee, M. Kim, H. Jung, and M. Guizani, "Window function-based frequency diverse sub-arrays for randomized radiation enhancement," *IEEE Transactions on Vehicular Technology*, pp. 1–6, 2025.
- [3] U. Iqbal, S. Cho, H. Jung, and M. Guizani, "Performance analysis of physical layer security for over-the-air computation using distributed null-steering beamforming," *IEEE Communications Letters*, vol. 29, no. 2, pp. 303–307, 2025.
- [4] T. C. Lam, N.-S. Vo, M.-P. Bui, C. D. T. Thai, H. Jung, and V.-C. Phan, "Service time-aware caching, power allocation, and 3D trajectory optimised multimedia content delivery in UAV-assisted IoT networks," *IEEE Transactions on Vehicular Technology*, vol. 74, no. 4, pp. 6419–6432, 2025.
- [5] B. You, I.-H. Lee, H. Jung, T. Q. Duong, and H. Shin, "Secure 3D directional modulation using subarrays based on planar frequency diverse array with nonuniform frequency offsets," *IEEE Transactions on Communications*, vol. 73, no. 6, pp. 4017–4032, 2025.
- [6] J. Han, J.-B. Kim, I.-H. Lee, and H. Jung, "3-D sidelobe suppression for collaborative beamforming with uavs," *IEEE Wireless Communications Letters*, vol. 14, no. 3, pp. 796–800, 2025.
- [7] A. Umar, A. Umer, H. Jung, H. Abou-Zeid, A. A. Nasir, and S. A. Hassan, "High altitude edge computing-enabled integrated networks for 6G communications," *IEEE Communications Standards Magazine*, vol. 9, no. 2, pp. 7–14, 2025.
- [8] S. A. Ullah, S. A. Hassan, H. Abou-Zeid, H. K. Qureshi, H. Jung, A. Mahmood, M. Gidlund, M. A. Imran, and E. Hossain, "Convergence of MEC and DRL in non-terrestrial wireless networks: Key innovations, challenges, and future pathways," *IEEE Communications Surveys & Tutorials*, Early Access, 2025.
- [9] D. Kim, H. Jung, and I.-H. Lee, "DQN-based scheduling algorithm for beam-hopping LEO satellite communication systems," *IEEE Wireless Communications Letters*, vol. 14, no. 8, pp. 2401–2405, 2025.
- [10] D. Kim, H. Jung, I.-H. Lee, and D. Niyato, "Multibeam management and resource allocation for LEO satellite-assisted IoT networks," *IEEE Internet of Things Journal*, vol. 12, no. 12, pp. 19443–19458, 2025.
- [11] H. Noh, H. Jung, and J. Lee, "TN-NTN aggregation and unification in 6G," in 2024 15th International Conference on Information and Communication Technology Convergence (ICTC), 2024, pp. 1439–1440.
- [12] F. Rinaldi, H.-L. Maattanen, J. Torsner, S. Pizzi, S. Andreev, A. Iera, Y. Koucheryavy, and G. Araniti, "Non-terrestrial networks in 5G & beyond: A survey," *IEEE Access*, vol. 8, pp. 165 178–165 200, 2020.
- [13] W. Liu, X. Hou, J. Wang, L. Chen, and S. Yoshioka, "Uplink time synchronization method and procedure in Release-17 NR NTN," in 2022 IEEE 95th Vehicular Technology Conference: (VTC2022-Spring), 2022, pp. 1–5.
- [14] M. M. Saad, M. A. Tariq, M. T. R. Khan, and D. Kim, "Non-terrestrial networks: An overview of 3GPP Release 17 & 18," *IEEE Internet of Things Magazine*, vol. 7, no. 1, pp. 20–26, 2024.
- [15] J. Zhu, Y. Sun, and M. Peng, "Timing advance estimation in low earth orbit satellite networks," *IEEE Transactions on Vehicular Technology*, vol. 73, no. 3, pp. 4366–4382, 2024.
- [16] L. Ma, C. Park, X. Wang, P. Gaal, and A. R. Alvarino, "Uplink time synchronization for non-terrestrial networks," *IEEE Communications Magazine*, vol. 61, no. 7, pp. 114–118, 2023.
- [17] W.-Y. Yeo and D.-J. Lee, "Uplink time synchronization based on time drift measurements in non-terrestrial networks," *IEEE Access*, vol. 12, pp. 168 877–168 893, 2024.
- [18] F. Kunzi and O. Montenbruck, "Precise onboard time synchronization for LEO satellites," *NAVIGATION: Journal of the Institute of Navigation*, vol. 69, no. 3, 2022. [Online]. Available: https://navi.ion.org/content/69/3/navi.531